Microporous and Mesoporous Materials 165 (2013) 92–98

Contents lists available at SciVerse ScienceDirect

Microporous and Mesoporous Materials

journal homepage: www.elsevier.com/locate/micromeso

Targeted synthesis of micro–mesoporous hybrid material derived from octaphenylsilsesquioxane building units

Xiaofei Jing [a], Fuxing Sun [a], Hao Ren [a], Yuyang Tian [a], Mingyi Guo [a], Lina Li [a], Guangshan Zhu [a,b,*]

[a] State Key Laboratory of Inorganic Synthesis and Preparative Chemistry, Jilin University, Changchun 130012, China
[b] Queensland Micro- and Nanotechnology Centre, Griffith University, Queensland, 4111, Australia

ARTICLE INFO

Article history:
Received 5 June 2012
Received in revised form 24 July 2012
Accepted 26 July 2012
Available online 3 August 2012

Keywords:
Micro–mesoporous material
Hybrid material
Silsesquioxane
Suzuki reaction

ABSTRACT

A micro–mesoporous inorganic–organic hybrid material PAF-12, derived from octaphenylsilsesquioxane (OPS, $[C_6H_5(SiO_{1.5})]_8$) as basic building units, was successfully synthesized via Suzuki cross-coupling reaction. Thermogravimetric analysis (TGA) shows that PAF-12 is thermally stable up to 500 °C in air condition. According to Ar sorption isotherm, the network of PAF-12 shows classic type IV isotherm and also exhibits a sharp uptake at low relative pressures indicating micro–mesoporous texture. The pore size distribution of PAF-12 calculated from non-linear density functional theory (NLDFT) gives only two clear narrow peaks centered at 1.57 and 3.17 nm. To the best of our knowledge, PAF-12 is the first hybrid material containing both micropore and mesopore reported for silsesquioxane-based materials. Additionally, PAF-12 exhibits high adsorption abilities for organic chemical pollutants such as benzene and methanol. The effects of different solvent systems to synthesize PAF-12 were also investigated and the optimal condition was found out.

1. Introduction

Driven by potential applications such as gas storage, molecular separation and catalysis [1,2], investigations on porous materials have made great progress in recent years [3,4], especially the appearance of reticular chemistry has led to numerous practical and conceptual developments and makes the synthesis of new porous materials more targeted [5–9]. Since covalent organic frameworks (COFs) represented by Yaghi et al. [8], the developments of porous organic frameworks (POFs) are expeditious in the field of synthetic versatility and global properties. POFs derived wholly from light elements possess intrinsic microporosity which arises directly from the shape and rigidity of component. Furthermore, POFs materials are highly stable under rigorous conditions due to their nature of robust covalent bonds. Various POFs, such as COFs [8–11], polymers of intrinsic microporosity (PIMs) [12,13], conjugated microporous polymers (CMPs) [14–16], hyper-crosslinked polymers (HCPs) [17,18], crystalline triazine-based organic frameworks (CTFs) [19,20] and porous aromatic frameworks (PAFs) [21,22], have been created and synthesized successfully in the past decade, and they have brought major advances in porous materials domain. Presently, microporous POFs have attracted intense interests because of their intrinsic porosity and vital applications [23]. However, mesoporous POFs with regular pore size distribution are relatively scarce, which may satisfy applications in the fields of biotechnologies and macromolecules [24,25]. The expansion and decoration of the topological networks of inorganic materials especially zeolite topologies via selecting bigger building blocks and longer linkage units is proved to be effective and powerful strategy to produce highly mesoporous materials [26–29]. As a classic and critical family of porous materials, zeolites are widely used in the chemical industry as adsorbers, detergent builders and containers for confined materials [30,31]. Conceptually, varying the lengths of rigid linear linkages would not only retain a zeolite-like structural stability but also allow an efficient pore size extension from microporous to mesoporous [21].

To create porosity in POFs, the key points of the current method are the choice of the suitable building unit and the reaction medium [32]. OPS as an outstanding candidate [33] to assemble materials in three dimensions with perfect control of periodicity has attracted considerable attention due to its rigid cubic symmetry coupled with about 1 nm diameter. The hyper-branched architecture and ease of functionalization provide the possibility to tailor global properties at nanometer length scales. Also the combination of inorganic D4R building blocks and organic linkages would remarkably improve the mechanical property of skeleton compared to the pure organic polymers [34]. Recent investigations reported by Laine [35,36], Okubo [37,38] and ourselves [39] indicate that hybrid microporous materials by directly linking functionalized D4R with rigid linkers show partially crystalline which are rare in POFs assembled under kinetics controlled reaction. It is well known that D4R is the basic building unit in zeolites, and directly

* Corresponding author at: State Key Laboratory of Inorganic Synthesis and Preparative Chemistry, Jilin University, Changchun 130012, China. Tel.: +86 431 85168887; Fax: +86 431 85168331.
E-mail address: zhugs@jlu.edu.cn (G. Zhu).

1387-1811/$ - see front matter © 2012 Elsevier Inc. All rights reserved.
http://dx.doi.org/10.1016/j.micromeso.2012.07.048

connecting the D4R vertices with linear linkages would result in structures with LTA and ACO frameworks [40–42]. Extension of the linkage among the D4R building block would effectively increase the pore size of the structure to mesoporous range while maintain the topology. Palladium-catalyzed cross-coupling reactions [43] such as Sonogashira reaction and Suzuki reaction, are well developed for synthesis of POFs materials [44–47], which are verified to be powerful ways to realize these "blueprints". In this work, we presented synthesis and properties of a new micro–mesoporous PAF material, PAF-12. I_8OPS and 1,4-phenyldiboronic acid were employed to couple together via Suzuki cross-coupling reaction to form PAF-12. As expected in Scheme 1, extended frameworks for linking D4R units directly by linear phenyl units have a chance to afford a two-cage LTA net with space group *Pm-3m* and reticular ACO net with space group *Im-3m*, respectively. The 3D models were obtained with the Materials Studio simulation environment [48] employing MS Visualizer. Energy minimization and geometry optimization were performed using force-field calculations to obtain reasonable bond lengths and angles (see in Supplementary materials).

2. Experimental

2.1. Materials

OPS and ICl (1.0 M in CH_2Cl_2) was purchased from Meryer and Aldrich, respectively. Other starting materials were purchased from commercial suppliers without further purification. All organic solvents for reactions were distilled over appropriate drying reagents under Ar before employments. I_8OPS was prepared according to the previously reported method [33].

2.2. Synthesis of PAF-12

I_8OPS (200 mg, 98 μmol) and 1,4-phenyldiboronic acid (65 mg, 392 μmol) in dehydrated N,N-dimethylformamide (DMF, 6.5 mL) were mixed in a Pyrex ampoule and the mixture was degassed by three freeze–pump-thaw cycles. Then an aqueous solution of potassium carbonate (2.0 M, 0.85 mL) and Tetrakis(triphenylphosphine)palladium (10 mol%) were added into the solution in ampoule quickly and degassed by three freeze–pump-thaw cycles again. Then, the Pyrex ampoule was purged with Ar and sealed. The mixture was stirred at 150 °C for 36 h. After cooling to room temperature, the mixture was poured into water. Then the precipitate was collected by filtration, thoroughly washed by Soxhlet extractions for 24 h with H_2O, acetone, tetrahydrofuran (THF) and methylene dichloride, respectively, and dried under vacuum at 120 °C to give PAF-12 as an off-white powder (92% yield).

PAF-12–1,2 were synthesized in the similar condition described above but different solvents 1,4-dioxane, THF instead of DMF respectively. Yields: 94% (1,4-dioxane/H_2O: PAF-12–1), 99% (THF/H_2O: PAF-12–2). The samples for characterizations were activated under vacuum at 150 °C for 12 h before employments.

2.3. Physical measurements

The Fourier transform infrared spectroscopy (FTIR) spectra (film) were measured using a IFS 66 V/S Fourier transform infrared

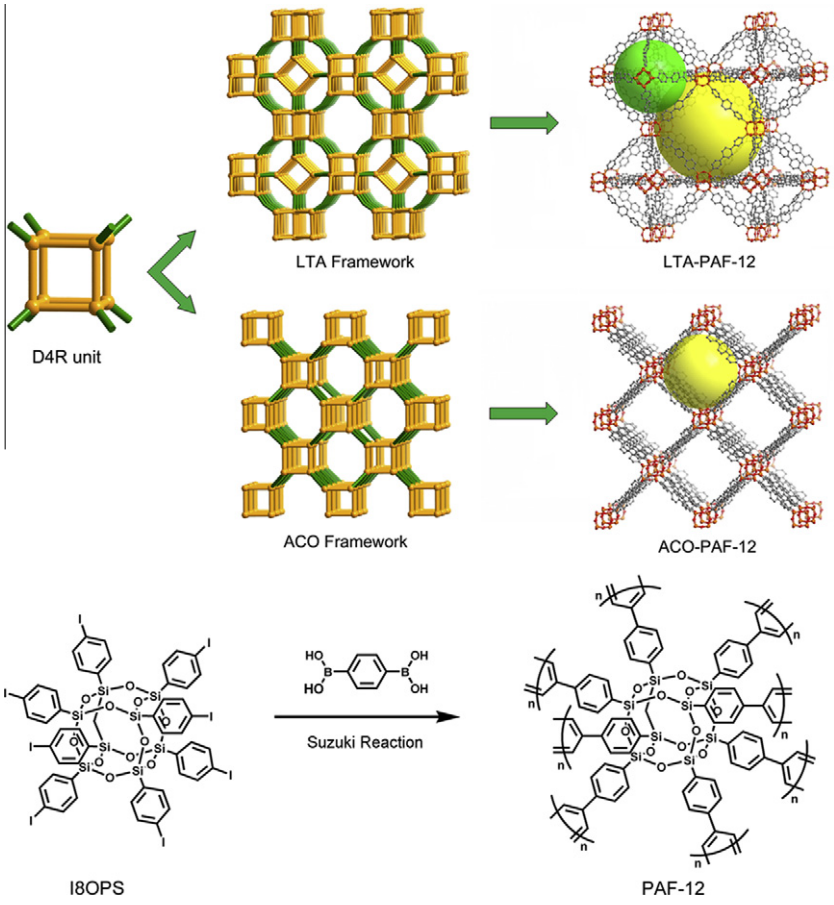

Scheme 1. The strategy of synthesis of a hybrid material PAF-12. Above: possible frameworks for linking D4R units directly and corresponding extended structures by replacing the linkage with linear triphenyl ring units (Si, O, C atoms are represented as orange, red, and gray, respectively). Below: synthetic pathway to PAF-12. H atoms are omitted for clarity. (For interpretation of color in Scheme 1, the reader is referred to the web version of this article.)

spectrometer. Solid-state ^{1}H–^{13}C CP/MAS NMR and ^{29}Si MAS NMR measurements were performed on a Bruker Avance III model 400 MHz NMR spectrometer at a MAS rate of 5 kHz. The powder X-ray diffraction (PXRD) was performed by a Riguku D/MAX2550 diffractometer using CuKα radiation, 40 kV, 200 mA with scanning rate of 0.06°/min (2θ). Scanning electron microscopy (SEM) analysis was performed on a JEOS JSM 6700. Transmission electron microscopy (TEM) was recorded using a JEOL JEM 3010 with an acceleration voltage of 300 kV. The Ar adsorption isotherm was measured on Quantachrome Autosorb-iQ analyzer. The organic molecules adsorption isotherms were measured on the Quantachrome Autosorb-iQ2-AG-VP. The thermogravimetric analysis (TGA) was performed using a Netzch Sta 449c thermal analyzer system at the heating rate of 10 °C /min in air condition. X-ray photoelectron spectroscopy (XPS) was performed using Thermo ESCALAB 250.

3. Results and discussion

The resulting hybrid material PAF-12 has high thermal and chemical stability and high surface area. According to Ar sorption isotherm, PAF-12 shows classic type IV isotherm indicating mesoporous texture. The pore size distribution of PAF-12 calculated from NLDFT is consistent with theoretically calculated pore size of the ideally proposed structure with LTA topology. Additionally, PAF-12 exhibits high adsorption abilities for organic chemical pollutants such as benzene and methanol.

3.1. Structure information of PAF-12

3.1.1. FTIR spectra

Comparisons of the FTIR spectra of two monomers (I_8OPS and 1,4-phenyldiboronic acid) and PAF-12 were performed to confirm the cross-coupling reaction proceeded as desired. As shown in Fig. 1, the disappearances of intense C–I bands (at 1005 cm^{-1}) of I_8OPS, C–B bands (at 1352 and 1403 cm^{-1}) and B–OH bands (at 3414 and 3292 cm^{-1}) of 1,4-phenyldiboronic acid [49], suggest successful completion of the reaction. Additionally, the presence of D4R and phenyl rings in PAF-12 framework is also confirmed by FTIR. The strong peak at 1056 cm^{-1} is ascribed to typical stretch of Si–O–Si, which is a proof of the D4R cages. The weak peaks at 1485 and 1163 cm^{-1} belonging to Aromatic C–H stretching vibrations and the peaks appeared at 1599 and 1386 cm^{-1} belonging to Aromatic C=C stretching vibrations indicate the phenyl rings in the PAF-12 network [50].

3.1.2. ^{1}H–^{13}C CP/MAS NMR and ^{29}Si MAS NMR

Further investigations on the local structure of PAF-12 were performed by solid-state ^{1}H–^{13}C CP/MAS NMR and ^{29}Si MAS NMR studies. In the ^{1}H–^{13}C CP/MAS NMR spectrum (Fig. 2a), two signals at δ = 136 and 127 ppm are resolved, which are corresponding to substituted and unsubstituted bridging phenyl carbons, respectively. The ^{29}Si NMR spectrum ((Fig. 2b) displays the predominant signal at δ = −78.9 ppm with a small shoulder at δ = −69.8 ppm and a weak signal at δ = −61.8 ppm which can be assigned to T^3, T^2 and T^1 units, respectively (T^n: $CSi(OSi)_n(OH)_{3-n}$) [38]. The appearance of T^1 and T^2 units indicates that small portion of the D4R cages collapsed during synthesis, and the broad peak centered at −105 ppm ascribed to the presence of Q_n ($Si(OSi)_n(OH)_{4-n}$) species suggests that Si–C bonds have been partially cleaved. Such destructions occurred during the reaction were probably due to the basic environment employed in the polymerization process. However, it is noteworthy that most of the D4R cages were retained in PAF-12 network.

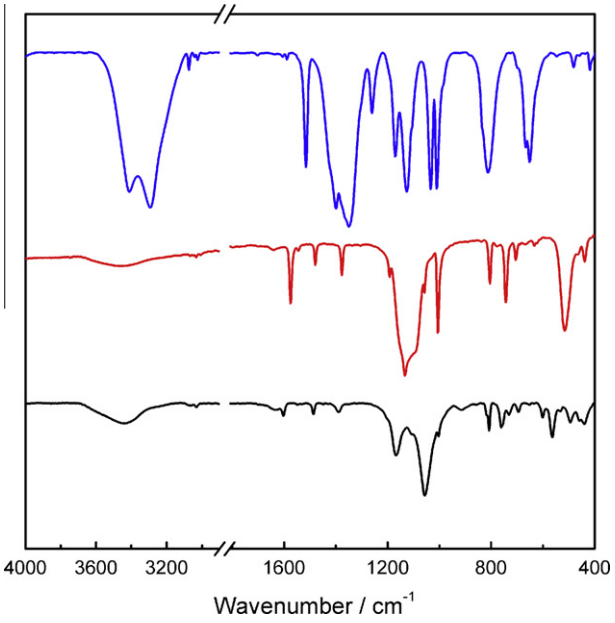

Fig. 1. FTIR spectra of PAF-12 (black), I_8OPS (red) and 1,4-phenyldiboronic acid (blue). (For interpretation of color in Fig. 1, the reader is referred to the web version of this article.)

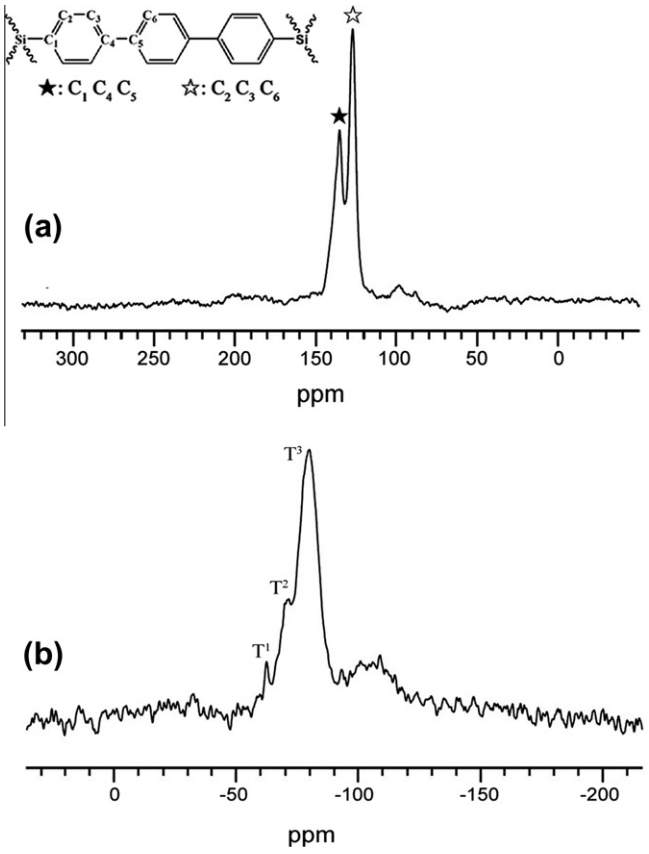

Fig. 2. (a). ^{1}H–^{13}C CP/MAS NMR spectrum; b). ^{29}Si MAS NMR spectrum of PAF-12 (T^n: $CSi(OSi)_n(OH)_{3-n}$).

3.1.3. Powder X-ray diffraction

In order to certify the long-range structure of PAF-12, PXRD was carried out. In contrast to the typical amorphous porous polymers[14,18,36,38], the PXRD pattern of PAF-12 shows four broad

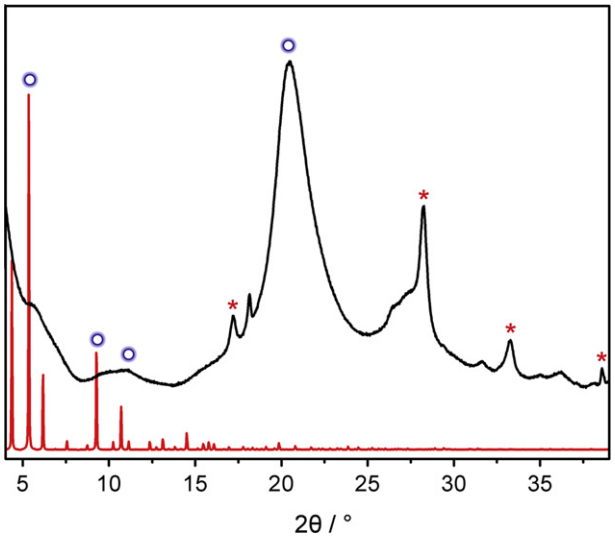

Fig. 3. The PXRD patterns of synthesized PAF-12 (black; circle: peaks arising from (200), (241) and (400) planes of LTA-PAF-12 model; asterisk: peaks arising from residual Pd compound) and the simulated LTA-PAF-12 framework (red). (For interpretation of the references to color in this figure legend, the reader is referred to the web version of this article.)

peaks at 2θ = 5.4°, 9.2°, 10.7° and 20.6° (Fig. 3). The peak at 5.4° is equivalent to a *d*-spacing distance of 1.63 nm, which is consistent with the peak at 1.57 nm of pore size distribution and the strong peak at 20.6°, corresponding to a *d*-spacing distance of 0.43 nm should be assigned to the D4R unit in the framework of PAF-12. This indicates that the obtained hybrid material has a certain long-range order although the degree of the order is not very high. From the combined XRD patterns, the three peaks at 5.4°, 9.2°, 10.7° in the experimental pattern (marked with blue circle in Fig. 3) can also be found in simulated XRD pattern, which arise from (200), (241) and (400) planes of LTA-PAF-12 model respectively (Fig. S1). Additionally, Pd compound which is hard to remove thoroughly is residual in PAF-12 and the sharp peaks marked with asterisk in Fig. 3 could be attributed to Pd compound.

3.1.4. Scanning electron microscopy

The morphology and size of PAF-12 were investigated by SEM measurement. As shown in Fig. 4, the powder of PAF-12 is amorphous and mostly micro-sized irregular blocks, and some are small nano-sized particles with the size of 400 nm.

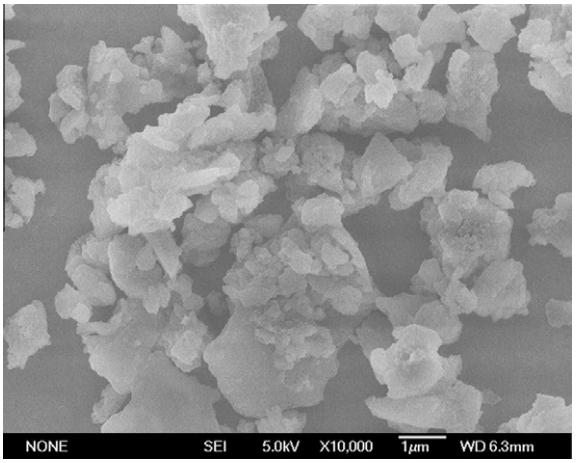

Fig. 4. SEM image of PAF-12.

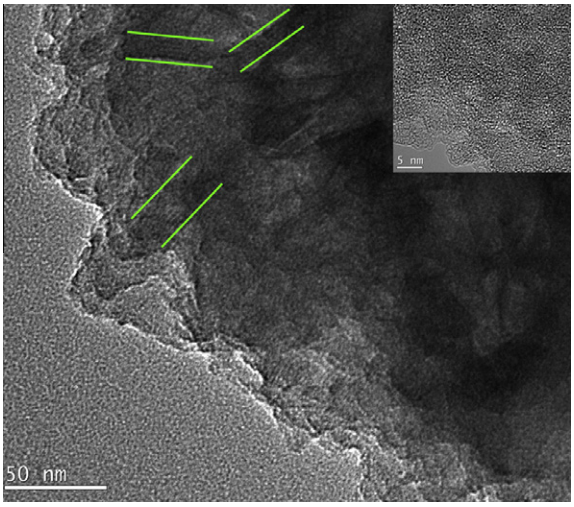

Fig. 5. TEM images of PAF-12 (insert: the magnified image).

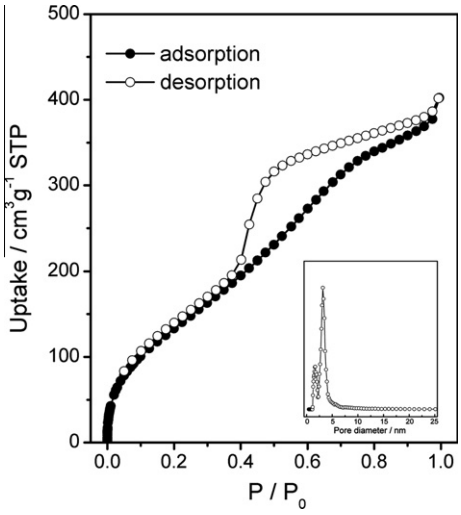

Fig. 6. Ar sorption isotherm and pore size distribution (insert) of PAF-12.

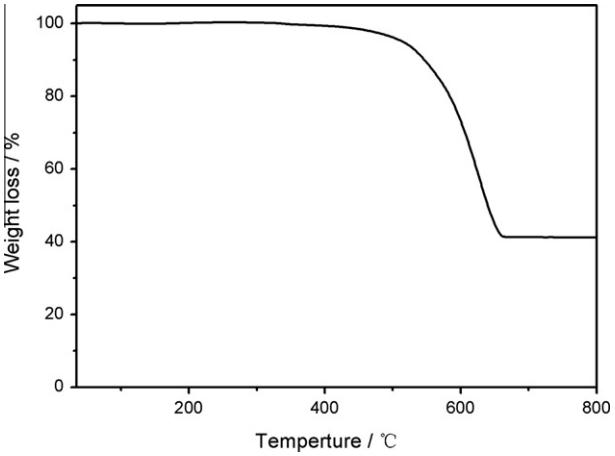

Fig. 7. TGA plot of PAF-12 under air condition.

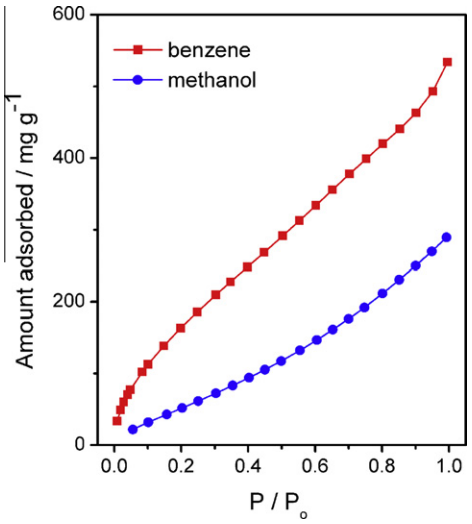

Fig. 8. Benzene and methanol vapor adsorption isotherms at 298 K.

3.1.5. Transmission electron microscopy

TEM investigations show a clearly porous texture. Obviously regular pore channels in local structure of PAF-12 (as the stripy areas marked between green lines in Fig. 5) were observed, and the width of these channels estimated by TEM is about 3 nm. Combining PXRD with TEM investigation, it implies that PAF-12 possesses a certain ordered texture.

3.2. Properties and application of PAF-12

3.2.1. Ar sorption measurements

The pore character of PAF-12 was studied by Ar sorption isotherm measured at 87 K. As indicated in Fig. 6, PAF-12 shows a classic type IV isotherm which is featured by a distinct hysteresis loop in the desorption branch and also exhibits a sharp uptake at low relative pressures, which might be an indicator for PAF-12 possessing both microporous and mesoporous texture. The apparent surface area of PAF-12 calculated from the Brunauer–Emmett–Teller (BET) model is 484 $m^2 g^{-1}$. and pore size distribution calculated from NLDFT gives two narrow peaks centered at 1.57 and 3.17 nm. As expected in Scheme 1, the diameters of two cages with extended LAT framework (LTA-PAF-12) are 1.61 and 3.12 nm respectively, and the extended ACO net (ACO-PAF-12) has only single pore with diameter 2.12 nm along (100). Therefore the pore size of PAF-12 is consistent with theoretically pore size of LTA-PAF-12, suggesting that PAF-12 might afford the LTA topology. Estimated from the amount of gas uptake at $P/P_0 = 0.99$, the total pore volume is 0.51 $cm^3 g^{-1}$.

3.2.2. Stability of PAF-12

TGA under air was performed to study the thermal stability of PAF-12. The framework does not collapse until 340 °C and has only 4% weight loss from 340 to 500 °C (Fig. 7). It reveals PAF-12 has high thermal stability, which is comparable to other POFs [12,21]. PAF-12 also has a high chemical stability and can not be dissolved or decomposed in common organic solvents, such as DMF, $CHCl_3$ THF, etc.

3.2.3. Liquid vapor adsorption

The high porosity and aromatic framework of PAF-12 make itself an outstanding candidate for adsorbing organic chemical pollutants, such as benzene and methanol [22,51]. As shown in Fig. 8, PAF-12 can absorb large amounts of benzene and methanol with values of 534 and 289 mg g^{-1} at saturation and 298 K respectively, superior to some MOF materials [52,53]. PAF-12 features a typical type-II adsorption isotherm for benzene sorption and a type-III adsorption isotherm for methanol sorption suggesting a stronger guest–host interaction of benzene than methanol, which can be due to the π-π interaction between the benzene molecule and the aromatic framework of PAF-12 [54]. These excellent sorption performances of PAF-12 promise greatly potential for the further environmental applications.

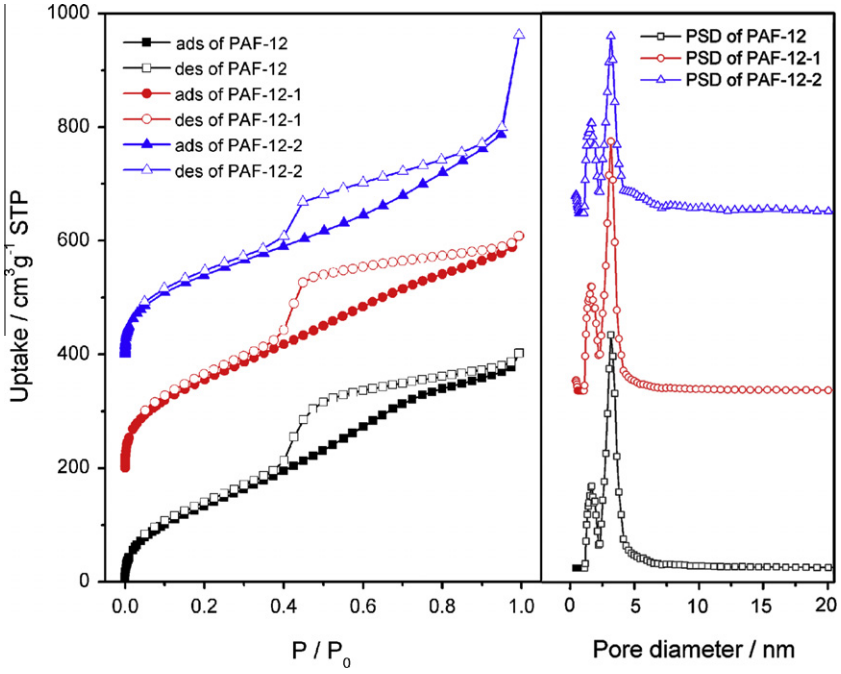

Fig. 9. Ar sorption isotherms (left: the isotherms have been offset by 200 units for the purpose of clarity) and pore size distributions (PSD, right) of samples synthesized in different solvent systems.

3.3. Effects of solvent choices to Suzuki cross-coupling reaction

As we known, the solvent choice for Suzuki cross-coupling reaction mainly includes DMF/H_2O, 1,4-dioxane/H_2O, THF/H_2O and methanol/H_2O systems [33,45,46]. In order to investigate the effects of different solvent systems to polymerizations, comparative reactions in 1,4-dioxane and THF were carried out at proper temperatures except methanol/H_2O system because of bad solubility of I_8OPS in methanol. Comparative FTIR spectra of materials synthesized in different solvent systems shows no obvious difference (Fig. S2), which indicate the cross-coupling reaction all proceeded as desired. To confirm the optimal condition, XPS was performed. In DMF/H_2O system no iodine end groups were detected (the average molar ratio of I/Si < 0.001), indicating that nearly all end groups have been reacted. In contrast, I/Si molar ratios of samples synthesized in the other two solvent systems are 0.097 (PAF-12–1) and 0.295 (PAF-12–2), respectively. These results indicate that the reaction in DMF/H_2O system proceeded more completely, suggesting DMF/H_2O system is better than 1,4-dioxane/H_2O and THF/H_2O systems for the syntehsis of PAF-12.

Ar sorption measurements of these samples show similar IV type isotherms (Fig. 9, left), and the values of BET apparent surface areas are not of much difference (Table S1). The pore size distributions derived from Ar adsorption isotherms (Fig. 9, right) are almost the same and show clearly two narrow peaks which strongly verify the reproducibility of Suzuki cross-coupling reaction and the proposed LTA net of PAF-12. The sorption isotherm of PAF-12–2 increased rapidly at $P/P_0 \approx 1.0$, which could be attributed to the surface adsorption of assembled small particles.

PXRD patterns of samples synthesized in different solvent systems (Fig. S3) show the same peaks at 5.4°, 9.2°, 10.7° and 20.6°, further indicating the excellent reproducibility of Suzuki reaction which is suitable for synthesis of POFs.

4. Conclusions

In conclusion, a micro–mesoporous inorganic–organic hybrid material, PAF-12, constructed from D4R building units was synthesized by I_8OPS and 1,4-phenyldiboronic acid via Suzuki cross-coupling reaction. PAF-12 has high thermal and chemical stability and high surface area. The Ar sorption isotherm shows the existence of micro- and mesopores in PAF-12 and the calculated pore size distribution of PAF-12 is consistent with that of the ideally proposed structure with LTA topology. Additionally, PAF-12 exhibits high adsorption abilities for organic chemical pollutants such as benzene and methanol. The presented study paves a novel strategy to explore mesoporous POF materials for practical application in biochemistry.

Acknowledgment

We are grateful for the financial support of National Basic Research Program of China (973 Program, grant nos. 2012CB821700), Major International (Regional) Joint Research Project of NSFC (Grant Nos. 21120102034) and NSFC (Grant Nos. 20831002).

Appendix A. Supplementary data

Supplementary data associated with this article can be found, in the online version, at http://dx.doi.org/10.1016/j.micromeso.2012.07.048.

References

[1] F. Schüth, K.S.W. Sing, J. Weitkamp, Handbook of Porous Solids, Wiley-VCH, Weinheim, 2002.
[2] M.E. Davis, Nature 417 (2002) 813–821.
[3] R. Dawson, A.I. Cooper, D.J. Adams, Prog. Polym. Sci. 37 (2012) 530–563.
[4] C. Sanchez, K.J. Shea, S. Kitagawa, Chem. Soc. Rev. 40 (2011) 471–472.
[5] O.M. Yaghi, M. O'Keeffe, M. Kanatzidis, J. Solid State Chem. 152 (2000) 1–2.
[6] M. O'Keeffe, M. Eddaoudi, H.L. Li, T. Reineke, O.M. Yaghi, J. Solid State Chem. 152 (2000) 3–20.
[7] O.M. Yaghi, M. O'Keeffe, N.W. Ockwig, H.K. Chae, M. Eddaoudi, J. Kim, Nature 423 (2003) 705–714.
[8] A.P. Cote, A.I. Benin, N.W. Ockwig, M. O'Keeffe, A.J. Matzger, O.M. Yaghi, Science 310 (2005) 1166–1170.
[9] A.P. Cote, H.M. El-Kaderi, H. Furukawa, J.R. Hunt, O.M. Yaghi, J. Am. Chem. Soc. 129 (2007) 12914–12915.
[10] S.Y. Ding, J. Gao, Q. Wang, Y. Zhang, W.G. Song, C.Y. Su, W. Wang, J. Am. Chem. Soc. 133 (2011) 19816–19822.
[11] X.S. Ding, J. Guo, X.A. Feng, Y. Honsho, J.D. Guo, S. Seki, P. Maitarad, A. Saeki, S. Nagase, D.L. Jiang, Angew. Chem., Int. Ed. 50 (2011) 1289–1293.
[12] P.M. Budd, B.S. Ghanem, S. Makhseed, N.B. McKeown, K.J. Msayib, C.E. Tattershall, Chem. Commun. (2004) 230–231.
[13] P.M. Budd, Science 316 (2007) 210–211.
[14] J.X. Jiang, F. Su, A. Trewin, C.D. Wood, N.L. Campbell, H. Niu, C. Dickinson, A.Y. Ganin, M.J. Rosseinsky, Y.Z. Khimyak, A.I. Cooper, Angew. Chem., Int. Ed. 46 (2007) 8574–8578.
[15] A.I. Cooper, Adv. Mater. 21 (2009) 1291–1295.
[16] R. Dawson, A. Laybourn, Y.Z. Khimyak, D.J. Adams, A.I. Cooper, Macromolecules 43 (2010) 8524–8530.
[17] C.D. Wood, B. Tan, A. Trewin, H.J. Niu, D. Bradshaw, M.J. Rosseinsky, Y.Z. Khimyak, N.L. Campbell, R. Kirk, E. Stockel, A.I. Cooper, Chem. Mater. 19 (2007) 2034–2048.
[18] C.D. Wood, B. Tan, A. Trewin, F. Su, M.J. Rosseinsky, D. Bradshaw, Y. Sun, L. Zhou, A.I. Cooper, Adv. Mater. 20 (2008) 1916–1921.
[19] P. Kuhn, M. Antonietti, A. Thomas, Angew. Chem., Int. Ed. 47 (2008) 3450–3453.
[20] P. Kuhn, A. Forget, D.S. Su, A. Thomas, M. Antonietti, J. Am. Chem. Soc. 130 (2008) 13333–13337.
[21] T. Ben, H. Ren, S.Q. Ma, D.P. Cao, J.H. Lan, X.F. Jing, W.C. Wang, J. Xu, F. Deng, J.M. Simmons, S.L. Qiu, G.S. Zhu, Angew. Chem., Int. Ed. 48 (2009) 9457–9460.
[22] H. Ren, T. Ben, E.S. Wang, X.F. Jing, M. Xue, B.B. Liu, Y. Cui, S.L. Qiu, G.S. Zhu, Chem. Commun. 46 (2010) 291–293.
[23] R. Dawson, E. Stockel, J.R. Holst, D.J. Adams, A.I. Cooper, Energy Environ. Sci. 4 (2011) 4239–4245.
[24] F. Muharnmad, M.Y. Guo, W.X. Qi, F.X. Sun, A.F. Wang, Y.J. Guo, G.S. Zhu, J. Am. Chem. Soc. 133 (2011) 8778–8781.
[25] L.H. Chen, G.S. Zhu, D.L. Zhang, H. Zhao, M.Y. Guo, S.B. Wei, S.L. Qiu, J. Mater. Chem. 19 (2009) 2013–2017.
[26] E.L. Spitler, B.T. Koo, J.L. Novotney, J.W. Colson, F.J. Uribe-Romo, G.D. Gutierrez, P. Clancy, W.R. Dichtel, J. Am. Chem. Soc. 133 (2011) 19416–19421.
[27] Y.L. Liu, V.C. Kravtsov, R. Larsen, M. Eddaoudi, Chem. Commun. (2006) 1488–1490.
[28] G. Ferey, C. Mellot-Draznieks, C. Serre, F. Millange, J. Dutour, S. Surble, I. Margiolaki, Science 309 (2005) 2040–2042.
[29] Q.R. Fang, G.S. Zhu, M. Xue, J.Y. Sun, Y. Wei, S.L. Qiu, R.R. Xu, Angew. Chem., Int. Ed. 44 (2005) 3845–3848.
[30] T. Kodaira, Y. Nozue, S. Ohwashi, T. Goto, O. Terasaki, Phys. Rev. B 48 (1993) 12245–12252.
[31] H. Van Bekkum, E.M. Flanigen, P.A. Jacobs, J.C. Jansen, Introduction to Zeolite Science and Practice, Elsevier, Amsterdam, 2001.
[32] D.Q. Yuan, W.G. Lu, D. Zhao, H.C. Zhou, Adv. Mater. 23 (2011) 3723–3725.
[33] M.F. Roll, M.Z. Asuncion, J. Kampf, R.M. Laine, ACS Nano. 2 (2008) 320–326.
[34] G. Kickelbick, Prog. Polym. Sci. 28 (2003) 83–114.
[35] M.F. Roll, J.W. Kampf, Y. Kim, E. Yi, R.M. Laine, J. Am. Chem. Soc. 132 (2010) 10171–10183.
[36] Y. Kim, K. Koh, M.F. Roll, R.M. Laine, A.J. Matzger, Macromolecules 43 (2010) 6995–7000.
[37] W. Chaikittisilp, A. Sugawara, A. Shimojima, T. Okubo, Chem. Mater. 22 (2010) 4841–4843.
[38] W. Chaikittisilp, A. Sugawara, A. Shimojima, T. Okubo, Chem. Eur. J. 16 (2010) 6006–6014.
[39] Y. Peng, T. Ben, J. Xu, M. Xue, X.F. Jing, F. Deng, S.L. Qiu, G.S. Zhu, Dalton Trans. 40 (2011) 2720–2724.
[40] M. O'Keeffe, O.M. Yaghi, Chem. Eur. J. 5 (1999) 2796–2801.
[41] S. Sugiyama, S. Yamamoto, O. Matsuoka, H. Nozoye, J. Yu, G. Zhu, S. Qiu, O. Terasaki, Microporous Mesoporous Mater. 28 (1999) 1–7.
[42] O. Delgado-Friedrichs, M. O'Keeffe, O.M. Yaghi, Phys. Chem. Chem. Phys. 9 (2007) 1035–1043.
[43] F. Diederich, P.J. Stang, Metal-catalyzed Cross-Coupling Reactions, Wiley-VCH, Weinheim, 2004.
[44] J.X. Jiang, A. Trewin, F.B. Su, C.D. Wood, H.J. Niu, J.T.A. Jones, Y.Z. Khimyak, A.I. Cooper, Macromolecules 42 (2009) 2658–2666.
[45] L. Chen, Y. Honsho, S. Seki, D.L. Jiang, J. Am. Chem. Soc. 132 (2010) 6742–6748.
[46] L. Chen, Y. Yang, D.L. Jiang, J. Am. Chem. Soc. 132 (2010) 9138–9143.

[47] Q. Chen, M. Luo, T. Wang, J.X. Wang, D. Zhou, Y. Han, C.S. Zhang, C.G. Yan, B.H. Han, Macromolecules 44 (2011) 5573–5577.
[48] Materials Studio simulation environment, version 4.4, Accelrys software Inc., San Diego, CA, USA.
[49] W.W. Simons, The Sadtler Handbook of Infrared Spectra, Bio-Rad Laboratories, Inc., Informatics Division, 1978.
[50] T. Heine, H.F. Santos, S. Patchkovskii, H.A. Duarte, J. Phys. Chem. A 111 (2007) 5648–5654.
[51] Y. Yuan, F.X. Sun, H. Ren, X.F. Jing, W. Wang, H.P. Ma, H.J. Zhao, G.S. Zhu, J. Mater. Chem. 21 (2011) 13498–13502.
[52] S. Hu, K.H. He, M.H. Zeng, H.H. Zou, Y.M. Jiang, Inorg. Chem. 47 (2008) 5218–5224.
[53] D.X. Xue, Y.Y. Lin, X.N. Cheng, X.M. Chen, Cryst. Growth Des. 7 (2007) 1332–1336.
[54] K. Seiichi, I. Tatsuo, A. Ikuo, Adsorption Science (2nd) [M], G.X. Li Transl. Chemical Industry Press, Beijing, 2005.